

Phenomenology of Two-Texture Zero Neutrino Mass Matrices

S. Dev,^y Sanjeev Kumar^y, Surender Verma^z and Shivani Gupta^x

Department of Physics, Himachal Pradesh University, Shimla 171005,
INDIA

Abstract

The generic predictions of two-texture zero neutrino mass matrices in the flavor basis have been examined especially in relation to the degeneracies between mass matrices within a class and interesting constraints on the neutrino parameters have been obtained. It is shown that the knowledge of the octant of θ_{23} , the sign of $\cos \delta$ and neutrino mass hierarchy can be used to lift these degeneracies.

1 Introduction

Mass matrices provide important tools for the investigation of the underlying symmetries and the resulting dynamics. The first step in this direction is the reconstruction of the neutrino mass matrix in the flavor basis. However, the reconstruction results in a large variety of possible structures of mass matrices depending strongly on the mass scale, mass hierarchy and the Majorana phases. However, the relatively weak dependence on some oscillation parameters (θ_{23} and δ) results in the degeneracy of possible neutrino mass matrices. The mass matrix for Majorana neutrinos contains nine physical parameters including the three mass eigenvalues, three mixing angles and the three CP-violating phases. The two squared-mass differences (m_{12}^2 and m_{13}^2) and the two mixing angles (θ_{12} and θ_{23}) have been measured in solar, atmospheric and reactor experiments. The third mixing angle θ_{13} and the Dirac-type CP-violating phase δ are expected to be measured in the forthcoming neutrino oscillation experiments. The possible measurement of the effective Majorana mass in neutrinoless double decay searches will provide an additional constraint on the remaining three neutrino parameters viz. the neutrino mass scale and two Majorana-type CP-violating phases. While

dev5703@yahoo.com

^ysanjeev3kumar@gmail.com

^zs.7verma@yahoo.co.in

^xshiroberts.1980@yahoo.co.in

the neutrino mass scale will be independently determined by the direct beta decay searches and cosmological observations, the two Majorana phases will not be uniquely determined from the measurement of effective Majorana mass even if the absolute neutrino mass scale is known. Under the circumstances, it is natural to employ other theoretical inputs for the reconstruction of the neutrino mass matrix. The possible form of these additional theoretical inputs are limited by the existing neutrino data. Several proposals have been made in the literature to restrict the form of the neutrino mass matrix and to reduce the number of free parameters which include presence of texture zeros [1, 2, 3, 4, 5], requirement of zero determinant [6], the zero trace condition [7] to name just a few. However, the current neutrino oscillation data are consistent only with a limited number of texture schemes [1, 2, 3, 4, 5]. In particular, the current neutrino oscillation data disallow all neutrino mass matrices with three or more texture zeros in the flavor basis. Out of the fifteen possible neutrino mass matrices with two texture zeros, only seven are compatible with the current neutrino oscillation data. The seven allowed two texture zero mass matrices have been classified into three categories. The two class A matrices of the types A_1 and A_2 give normal hierarchy (NH) of neutrino masses. The class B matrices of types B_1, B_2, B_3 and B_4 yield a quasi-degenerate (QD) spectrum of neutrino masses. The single class C matrix corresponds to inverted hierarchy (IH) of neutrino masses.

In the absence of a significant breakthrough in the theoretical understanding of the fermion flavors, the phenomenological approaches are bound to play a crucial role in interpreting new experimental data on quark and lepton mixing. These approaches are expected to provide useful hints towards unraveling the dynamics of fermion mass generation, CP violation and identification of possible underlying symmetries of the lepton flavors from which realistic models of lepton mass generation and flavor mixing could be, hopefully, constructed.

Even though the grand unification on its own does not shed any light on the flavor problem, the Grand Unified Theories (GUTs) provide the optimal framework in which possible solutions to the flavor problem could be embedded. This is because the GUTs predict definite group theoretical relations between the fermion mass matrices. For this purpose, it is useful to find out possible leading order forms of the neutrino mass matrix in a basis in which the charged lepton mass matrix is diagonal. Such forms of neutrino mass matrix provide useful hints for model building which will eventually shed important light on the dynamics of lepton mass generation and flavor mixing. For example, a phenomenologically favored texture of quark mass matrix has been presented earlier [8]. In the spirit of quark-lepton similarity, the same texture has been prescribed for the charged lepton and Dirac neutrino mass matrices. The same texture for the right handed neutrino mass matrix in the see-saw mechanism might follow from universal flavor symmetry hidden in a more fundamental theory of mass generation. Thus, the texture zeros in different positions of the neutrino mass matrix, in particular and fermion mass matrices, in general could be consequence of an underlying symmetry [9, 10]. Such universal textures of fermion mass matrices can, theoretically, be obtained in the context of GUTs based on $SO(10)$ [11]. Moreover, neutrino mass matrices with texture zeros have important implications for leptogenesis [12].

In the present work, we examine phenomenological implications of all possible neutrino mass matrices with two texture zeros. Neutrino mass matrices within a class were thought

to have identical phenomenological consequences [1, 2, 3] leading to degeneracy of mass matrices within a class. Thus, there is a two-fold degeneracy in class A while the neutrino mass matrices of class B exhibit an eight-fold degeneracy since normal/inverted hierarchies are practically indistinguishable because of quasi-degenerate spectrum of neutrino masses in this class. We study this degeneracy in detail and discuss possible ways to lift this degeneracy. It is found that the deviation of atmospheric mixing from maximality and the quadrant of the Dirac-type CP-violating phase can be used to distinguish the mass matrices within a class. We, also, note that the determination of hierarchy will have important implications for class B neutrino mass matrices. The prospects for the measurement of θ_{13} for class A neutrino mass matrices are quite optimistic since a definite lower bound on θ_{13} is obtained for this class. For neutrino mass matrices of class B, CP-violation will be near maximal if θ_{13} is large. Definite lower bounds on the effective Majorana mass M_{ee} are obtained for neutrino mass matrices of class B and C. Class D of neutrino mass matrices is disallowed in our analysis.

2 Neutrino mass matrix

The neutrino mass matrix, M , can be parameterized in terms of three neutrino mass eigenvalues (m_1, m_2, m_3), three neutrino mixing angles ($\theta_{12}, \theta_{23}, \theta_{13}$) and one Dirac-type CP violating phase, δ . If neutrinos are Majorana particles then there are two additional CP violating phases, α, β , in the neutrino mixing matrix. The complex symmetric mass matrix M can be diagonalized by a complex unitary matrix V :

$$M = VM^{\text{diag}}V^T \quad (1)$$

where $M^{\text{diag}} = \text{Diag}(m_1; m_2; m_3)$. The neutrino mixing matrix V [13] can be written as

$$V = U P = \begin{pmatrix} 0 & c_{12}c_{13} & s_{12}c_{13} & s_{13}e^{-i\delta} & 1 & 0 & 0 & 1 \\ c_{12}c_{23} & c_{12}s_{23}s_{13}e^{i\alpha} & c_{12}c_{23} & s_{12}s_{23}s_{13}e^{i\alpha} & c_{23}c_{13} & c_{23}s_{13} & 0 & e^{i\beta} \\ s_{12}s_{23} & c_{12}s_{23}s_{13}e^{i\alpha} & s_{12}s_{23} & c_{12}c_{23}s_{13}e^{i\alpha} & c_{23}s_{13} & c_{23}c_{13} & 0 & 0 \\ 0 & 0 & 0 & 0 & 0 & 0 & e^{i(\beta+\gamma)} & 0 \end{pmatrix}; \quad (2)$$

where $s_{ij} = \sin \theta_{ij}$ and $c_{ij} = \cos \theta_{ij}$. The matrix V is called the neutrino mixing matrix or PMNS matrix. The matrix U is the lepton analogue of the CKM quark mixing matrix and P contains the two Majorana phases.

The elements of the neutrino mass matrix can be calculated from Eq. (1). Some of the elements of M , which can be equated to zero in the various allowed texture zero schemes, are given by

$$M_{ee} = c_{13}^2 c_{12}^2 m_1 + c_{13}^2 s_{12}^2 m_2 e^{2i\alpha} + s_{13}^2 m_3 e^{2i\beta}; \quad (3)$$

$$M_{e\mu} = c_{13} s_{13} s_{23} e^{i\alpha} (e^{2i\beta} m_3 - s_{12}^2 e^{2i\alpha} m_2) - c_{12} c_{23} s_{12} (m_1 - e^{2i\alpha} m_2) - c_{12}^2 s_{13} s_{23} e^{i\alpha} m_1 g; \quad (4)$$

$$M_{e\tau} = c_{13} s_{13} c_{23} e^{i\alpha} (e^{2i\beta} m_3 - s_{12}^2 e^{2i\alpha} m_2) + c_{12} s_{23} s_{12} (m_1 - e^{2i\alpha} m_2) - c_{12}^2 s_{13} c_{23} e^{i\alpha} m_1 g; \quad (5)$$

$$M_{\mu\mu} = m_1 (c_{23} s_{12} + e^{i\alpha} c_{12} s_{13} s_{23})^2 + e^{2i\alpha} m_2 (c_{12} c_{23} - e^{i\alpha} s_{12} s_{13} s_{23})^2 + e^{2i(\beta+\gamma)} m_3 c_{13}^2 s_{23}^2 \quad (6)$$

Type	Constraining Eqs.
A ₁	$M_{ee} = 0, M_e = 0$
A ₂	$M_{ee} = 0, M_e = 0$
B ₁	$M_e = 0, M_{\mu\mu} = 0$
B ₂	$M_e = 0, M_{\mu\mu} = 0$
B ₃	$M_e = 0, M_{\mu\mu} = 0$
B ₄	$M_e = 0, M_{\mu\mu} = 0$
C	$M_{\mu\mu} = 0, M_{\tau\tau} = 0$
D ₁	$M_{\mu\mu} = 0, M_{\tau\tau} = 0$
D ₂	$M_{\mu\mu} = 0, M_{\tau\tau} = 0$

Table 1: Allowed two texture zero mass matrices.

and

$$M_e = m_1 (s_{23} s_{12} - e^{i\delta} c_{12} s_{13} c_{23})^2 + e^{2i\delta} m_2 (c_{12} s_{23} + e^{i\delta} s_{12} s_{13} c_{23})^2 + e^{2i(\delta + \phi)} m_3 c_{13}^2 c_{23}^2. \quad (7)$$

It will be helpful to note from Eqs. (4-7) that the transformation

$$T = \begin{pmatrix} 1 & & \\ & \frac{1}{2} & \\ & & 1 \end{pmatrix} \quad (8)$$

transforms M_e to M_e and $M_{\mu\mu}$ to $M_{\mu\mu}$. Therefore, if M_e vanishes for θ_{23} and δ , then M_e vanishes for $\frac{\theta_{23}}{2}$ and $\delta + \phi$. Similarly, if $M_{\mu\mu}$ vanishes for θ_{23} and δ , then $M_{\mu\mu}$ vanishes for $\frac{\theta_{23}}{2}$ and $\delta + \phi$. This fact can be, gainfully, used for distinguishing the subcategories of neutrino mass matrices within a class.

3 Two texture zeros

The neutrino mass matrix, M_e , in the charged lepton basis is given by Eq. (1). Out of the fifteen possible patterns for two texture zeros in M_e , the seven possibilities [1, 2], which are found to be consistent with the current neutrino oscillation data, are listed in Table 1. In addition, we have, also, included the two mass matrices of class D in the list. These mass matrices were disallowed in some of the earlier analyses [1, 2]. However, it was found in a subsequent detailed numerical analysis by Guo and Xing [3] that the neutrino mass matrices of class D are, marginally, allowed. The expressions for the vanishing elements in different two-zero texture schemes have been listed in Eqs. (4-7).

The transformation T defined in Eq. (8) transforms neutrino mass matrices of type A₁ to A₂ and neutrino mass matrices of type B₁ (B₄) to B₂ (B₃). Therefore, the predictions for neutrino mass matrices of types A₁ and A₂ will be identical for all neutrino parameters except θ_{23} and/or δ . Similarly, the predictions of neutrino mass matrices for all the four types of mass matrices in class B will be identical for all neutrino parameters except θ_{23} and/or δ . However, the different types of mass matrices will have different predictions for the octant of θ_{23} and the sign of $\cos \delta$.

The two texture zeros in the neutrino mass matrix give two complex equations viz.

$$M_{ab} = 0; M_{pq} = 0 \quad (9)$$

where a, b, p and q can take values e, μ and τ . Eqs. (9) can, also, be written as

$$m_1 U_{a1} U_{b1} + m_2 U_{a2} U_{b2} e^{2i\alpha} + m_3 U_{a3} U_{b3} e^{2i(\alpha + \beta)} = 0 \quad (10)$$

and

$$m_1 U_{p1} U_{q1} + m_2 U_{p2} U_{q2} e^{2i\alpha} + m_3 U_{p3} U_{q3} e^{2i(\alpha + \beta)} = 0 \quad (11)$$

where U has been defined in Eq. (2). These two complex equations involve nine physical parameters $m_1, m_2, m_3, \theta_{12}, \theta_{23}, \theta_{13}$ and CP-violating phases α, β , and γ . The two mixing angles (θ_{12}, θ_{23}) and two mass-squared differences (m_{12}^2, m_{23}^2) are known from the solar, atmospheric and reactor neutrino experiments. The masses m_2 and m_3 can be calculated from the mass-squared differences m_{12}^2 and m_{23}^2 using the relations

$$m_2 = \sqrt{m_1^2 + m_{12}^2} \quad (12)$$

and

$$m_3 = \sqrt{m_2^2 + m_{23}^2} \quad (13)$$

Thus, we have two complex relations relating five unknown parameters viz. $m_1, \theta_{13}, \alpha, \beta$, and γ . Therefore, if one out of these five parameters is assumed, other four parameters can be predicted. Thus, neutrino mass matrices with two texture zeros in the flavor basis have strong predictive power.

Solving Eqs. (10) and (11) simultaneously, we obtain

$$\frac{m_1}{m_3} e^{-2i\alpha} = \frac{U_{p3} U_{q3} U_{a2} U_{b2}}{U_{a1} U_{b1} U_{p2} U_{q2}} \frac{U_{a3} U_{b3} U_{p2} U_{q2}}{U_{a2} U_{b2} U_{p1} U_{q1}} e^{2i(\alpha + \beta)} \quad (14)$$

and

$$\frac{m_1}{m_2} e^{-2i\alpha} = \frac{U_{p2} U_{q2} U_{a3} U_{b3}}{U_{a1} U_{b1} U_{p3} U_{q3}} \frac{U_{a2} U_{b2} U_{p3} U_{q3}}{U_{a3} U_{b3} U_{p1} U_{q1}} \quad (15)$$

Using Eqs. (14) and (15), the two mass ratios $\frac{m_1}{m_2}; \frac{m_1}{m_3}$ and Majorana phases (α, β) can be written as

$$\frac{m_1}{m_2} = \frac{U_{p2} U_{q2} U_{a3} U_{b3}}{U_{a1} U_{b1} U_{p3} U_{q3}} \frac{U_{a2} U_{b2} U_{p3} U_{q3}}{U_{a3} U_{b3} U_{p1} U_{q1}} \quad (16)$$

$$\frac{m_1}{m_3} = \frac{U_{p3} U_{q3} U_{a2} U_{b2}}{U_{a1} U_{b1} U_{p2} U_{q2}} \frac{U_{a3} U_{b3} U_{p2} U_{q2}}{U_{a2} U_{b2} U_{p1} U_{q1}} \quad (17)$$

$$= \frac{1}{2} \arg \frac{U_{p2} U_{q2} U_{a3} U_{b3}}{U_{a1} U_{b1} U_{p3} U_{q3}} \frac{U_{a2} U_{b2} U_{p3} U_{q3}}{U_{a3} U_{b3} U_{p1} U_{q1}} \quad (18)$$

and

$$= \frac{1}{2} \arg \frac{U_{p3} U_{q3} U_{a2} U_{b2}}{U_{a1} U_{b1} U_{p2} U_{q2}} \frac{U_{a3} U_{b3} U_{p2} U_{q2}}{U_{a2} U_{b2} U_{p1} U_{q1}} \quad (19)$$

Eqs. (18) and (19) give the Majorana phases α_1 and α_2 in terms of θ_{13} and δ since m_{12}^2 and m_{23}^2 are known experimentally. Similarly, Eqs. (16) and (17) give the mass ratios $\frac{m_1}{m_2}; \frac{m_1}{m_3}$ as functions of θ_{13} and δ . Since, m_{12}^2 and m_{23}^2 are known experimentally, the values of mass ratios $\frac{m_1}{m_2}; \frac{m_1}{m_3}$ from Eqs. (16) and (17) can be used to calculate m_1 . This can be done by inverting Eqs. (12) and (13) to obtain the two values of m_1 , viz.

$$m_1 = \frac{m_1}{m_2} \sqrt{\frac{m_{12}^2}{1 - \frac{m_1}{m_2}}}$$
 (20)

and

$$m_1 = \frac{m_1}{m_3} \sqrt{\frac{m_{12}^2 + m_{23}^2}{1 - \frac{m_1}{m_3}}}$$
 (21)

The two values of m_1 obtained above from the mass ratios $\frac{m_1}{m_2}$ and $\frac{m_1}{m_3}$, respectively, must be equal. Thus, we can constrain (θ_{13}, δ) plane using the experimental inputs for m_{12}^2 , m_{23}^2 , θ_{12} and θ_{23} . The Dirac-type CP violating phase, δ , is given full variation from 0° to 360° and θ_{13} is varied from zero to its upper bound from CHOOZ experiment. We use the current best fit values of the oscillation parameters with 1, 2 and 3 σ [4] errors given below :

$$\begin{aligned} m_{12}^2 &= 7.9^{+0.3; 0.6; 1.0}_{-0.3; -0.6; -0.8} \times 10^5 \text{ eV}^2 ; \\ m_{23}^2 &= 2.6^{+0.2; 0.4; 0.6}_{-0.2; -0.4; -0.6} \times 10^3 \text{ eV}^2 ; \\ s_{12}^2 &= 0.30^{+0.02; 0.06; 0.10}_{-0.02; -0.04; -0.06} ; \\ s_{23}^2 &= 0.50^{+0.06; 0.13; 0.18}_{-0.05; -0.12; -0.16} ; \\ s_{13}^2 &< 0.012; 0.025; 0.040 ; \end{aligned}$$
 (22)

Here, $^{+0}_{-0}$ ($^{+0}_{-0}$) sign with the value of m_{23}^2 is for normal (inverted) hierarchy. The analysis [14] incorporates not only the latest long baseline data for m_{13}^2 from the MINOS collaboration [15] but also the updated KamLAND and SNO data [16]. We vary the oscillation parameters within their 1, 2 and 3 σ C.L. ranges with uniform distributions and calculate their predictions at various confidence levels. However, we report the correlations plots at 1 σ C.L.. We, also, calculate the Jarlskog rephasing invariant quantity [18]

$$J = s_{12}s_{23}s_{13}c_{12}c_{23}c_{13}^2 \sin \delta$$
 (23)

for the allowed parameter space.

In our numerical analysis outlined above, the two squared-mass differences (m_{12}^2 and m_{23}^2) enter as two independent experimental inputs while the earlier analyses [1, 2, 3] require the ratio of two known mass-squared differences

$$R = \frac{m_{12}^2}{m_{23}^2} = \frac{1 - \left(\frac{m_1}{m_2}\right)^2}{1 - \left(\frac{m_1}{m_3}\right)^2}$$
 (24)

Type	$\frac{m_1}{m_2}$	$\frac{m_1}{m_3}$		
A ₁	\tan^2_{12}	$\tan_{12} \tan_{23} \sin_{13}$	$n + \frac{1}{2}$	$+\frac{1}{2} = n$
A ₂	\tan^2_{12}	$\frac{\tan_{12} \sin_{13}}{\tan_{23}}$	$n + \frac{1}{2}$	$+\frac{1}{2} = (n + \frac{1}{2})$
B ₁	1	\tan^2_{23}	n	$+\frac{1}{2} = (n + \frac{1}{2})$
B ₂	1	$\frac{1}{\tan^2_{23}}$	n	$+\frac{1}{2} = (n + \frac{1}{2})$
B ₃	1	\tan^2_{23}	n	$+\frac{1}{2} = (n + \frac{1}{2})$
B ₄	1	$\frac{1}{\tan^2_{23}}$	n	$+\frac{1}{2} = (n + \frac{1}{2})$
C	$\frac{1}{\tan^2_{12}}$	$\frac{1}{\tan_{12} \tan_{23} \sin_{13}}$	$n + \frac{1}{2}$	-
D ₁	$\frac{1}{\tan^2_{12}}$	$\frac{\tan_{23}}{\tan_{12} \sin_{13}}$	n	$+\frac{1}{2} = (n + \frac{1}{2})$
D ₂	$\frac{1}{\tan^2_{12}}$	$\frac{1}{\tan_{23} \tan_{12} \sin_{13}}$	$n + \frac{1}{2}$	$+\frac{1}{2} = n$

Table 2: Zeroth order approximations for neutrino mass matrices with two texture zeros.

to lie in the experimentally allowed range in order to constrain the other neutrino parameters. Our analysis makes direct use of the two mass-squared differences and has more constraining power whereas the earlier analyses which make use of the ratio R lose some of the constraining power because this procedure does not use the full experimental information currently available with us in the shape of two mass-squared differences. Moreover, since R is a function of mass ratios, it does not depend upon the absolute neutrino mass scale. It is obvious that the two mass ratios $\frac{m_1}{m_2}$ and $\frac{m_1}{m_3}$ may yield the experimentally allowed values of R [Eq. (24)] for mutually inconsistent values of m_1 [Eqs. (20) and (21)]. Such mass ratios were allowed in the earlier analyses based upon R [1, 2, 3]. However, our analysis selects only those mass ratios for which the values of m_1 obtained from Eqs. (20) and (21) are identical and the ratio R for these values of the mass ratios is automatically restricted to lie in the allowed experimental range. Moreover, the definition of R

$$R = \frac{m_{12}^2}{m_{23}^2} = \frac{jn_{22}^2 m_{11}^2}{jn_{33}^2 m_{22}^2} \quad (25)$$

used in many earlier analyses does not make use of the knowledge of solar mass hierarchy to constrain the neutrino parameter space. Our analysis disallows the class D of two-texture zero neutrino mass matrices which has been marginally allowed by Guo and Xing [3].

4 Results and discussion

In this section, we shall present the results of our numerical analysis for neutrino mass matrices of classes A, B and C based upon the approach described in the previous section. However, it will be helpful to know the Taylor series expansion of Eqs. (16-19) in the powers of s_{13} to appreciate the numerical results. The zeroth order terms of the Taylor series expansion have been tabulated in Table 2.

C.L.	m_1 (10^{-3}eV)	(deg)	(deg)	θ_{13} (deg)	J
1	2:6 – 4:5	83 – 97	80 – 80	5:2 – 6:3	0:025 – 0:025
2	2:1 – 8:9	77 – 103	90 – 90	4:2 – 9:1	0:037 – 0:037
3	1:7 – 13:4	73 – 107	90 – 90	3:3 – 11:5	0:046 – 0:046

Table 3: The predictions for neutrino mass matrices of class A.

1 predictions	θ_{13}
A_1	$150^\circ - 150^\circ$ $41:8^\circ - 48:2^\circ$
A_2	$30^\circ - 330^\circ$ $41:8^\circ - 48:2^\circ$

Table 4: The predictions for θ_{13} and θ_{23} for neutrino mass matrices of types A_1 and A_2 .

4.1 Class A

It can be seen from Table 2 that both the mass ratios $\frac{m_1}{m_2}; \frac{m_1}{m_3} \ll 1$ for neutrino mass matrices of class A. So, neutrino mass matrices of class A give hierarchical spectrum of neutrino masses. This case has, already, been analyzed analytically [5] and, here, we shall discuss the earlier results only for the sake of completeness.

The results for m_1 , θ_{12} , θ_{13} and J for class A mass matrices have been summarized in Table 3 at various confidence levels. These quantities are the same for mass matrices of types A_1 and A_2 . It can be seen from Table 3 that the 3 σ lower bound on θ_{13} is $3:3^\circ$. The range for the Majorana-type CP-violating phase θ_{12} at 1 C.L. is found to be $80^\circ - 80^\circ$. However, if the neutrino oscillation parameters are allowed to vary beyond their present 1.2 C.L. ranges, the full range for θ_{12} ($90^\circ - 90^\circ$) is allowed. At one standard deviation, the allowed range of θ_{12} is ($150^\circ - 150^\circ$) for type A_1 and ($30^\circ - 330^\circ$) for type A_2 and the allowed range of θ_{23} is ($41:8^\circ - 48:2^\circ$) for type A_1 and A_2 [Table 4]. Just like θ_{12} , no constraint on θ_{23} is obtained above 1.2 C.L. The accuracies of the oscillation parameters required to distinguish between the theoretical predictions of neutrino mass matrices of types A_1 and A_2 depend on the upper bound on θ_{13} . With the current precision of the oscillation parameters, the neutrino mass matrices of types A_1 and A_2 can be distinguished at 1, 2 and 3 C.L. for $\theta_{13} < 5:7^\circ; 5:2^\circ$ and $4:8^\circ$ respectively.

Fig. 1 (identical for A_1 and A_2) depicts the correlation plots of m_1 , θ_{12} and J at one standard deviation. Fig. 1 (a) shows θ_{12} as a function of m_1 and Fig. 1 (b) shows J as a function of m_1 . The large spread in the (m_1, θ_{12}) plot is due to the errors in the neutrino oscillation parameters. However, there is a very strong correlation between θ_{12} and J as indicated in Table 2. Such a correlation between the Majorana phases was noted earlier [3]. However, full ranges ($90^\circ - 90^\circ$) are allowed for the two Majorana phases in that analysis [3]. In contrast, we obtain a very narrow range for the Majorana phase θ_{12} around 90° [cf. Table 3]. Similarly, the Majorana phase θ_{23} is, also, constrained if the oscillation parameters are limited to their 1 σ ranges. Fig. 1 (c) depicts the correlation between J and m_1 .

In Fig. 2, we depict the correlation plots of θ_{12} and θ_{23} with θ_{13} for matrices of types A_1 (left

panel) and A_2 (right panel). We, also, show the correlation plots of θ_{12} and θ_{23} with one another as well as with θ_{13} in Fig. 2. The Dirac-type CP-violating phase δ is, strongly, correlated with the Majorana-type CP-violating phase α [Cf. Table 2]. It can be seen from (θ_{12}, δ) correlation plots [Fig. 2(a) and 2(b)] and (θ_{23}, δ) correlation plots [Fig. 2(c) and 2(d)] that there are small deviations in the values of δ around 90° and the correlation between θ_{12} and δ is, almost, linear. The fact that $\alpha + 2\beta \approx 0^\circ$ for A_1 type mass matrices and $\alpha + 2\beta \approx 180^\circ$ for A_2 type mass matrices [cf. Table 2] is apparent from the (θ_{12}, δ) correlation plots [Fig. 2(c) and 2(d)]. The (θ_{12}, δ) correlation was noted earlier by Xing [2] in its approximate form in a different parameterization. The $(\theta_{12}, \theta_{23})$ plots, clearly, illustrate the point that the neutrino mass matrices of types A_1 and A_2 prefer different regions on the $(\theta_{12}, \theta_{23})$ plane. This is contrary to the analysis done by Xing [3] where no constraints on θ_{12} and θ_{23} have been obtained. In fact, this feature is crucial for distinguishing mass matrices of types A_1 and A_2 which were found to be degenerate in the earlier analyses [1, 2, 3]. The constraints on θ_{12} and θ_{23} are very sensitive to the values of θ_{13} . For the values of θ_{13} smaller than 1 CHOOZ bound, the constraints on θ_{12} and θ_{23} become stronger which can be seen from the $(\theta_{13}, \theta_{23})$ and $(\theta_{13}, \theta_{12})$ correlation plots [Figures 2(g-j)]. For example, if $\theta_{13} > 5.6^\circ$, then $\theta_{23} > 46^\circ$ (above maximal) for type A_1 and $\theta_{23} < 44^\circ$ (below maximal) for type A_2 . It can, also, be seen from the $(\theta_{13}, \theta_{23})$ correlation plots in Fig. 2 that the deviation of θ_{23} from maximality is larger for smaller values of θ_{13} . Therefore, if future experiments measure θ_{13} below its present 1 σ bound, the neutrino mass matrices of types A_1 and A_2 will have different predictions for θ_{12} and θ_{23} with no overlap. However, it would be difficult to differentiate between matrices of types A_1 and A_2 if θ_{13} is found to be above its present 1 σ range. As noted earlier, different quadrants for δ are selected for neutrino mass matrices of types A_1 and A_2 . It can, also, be seen in Fig. 2 that the points $\delta = 0^\circ$ are ruled out implying that neutrino mass matrices of class A are necessarily CP-violating. This feature is, also, apparent in Fig. 2 which depict J as a function of δ for types A_1 [Fig. 2(k)] and A_2 [Fig. 2(l)].

4.2 Class B

It can be seen from Table 2 that the mass ratios $\frac{m_1}{m_2}$ and $\frac{m_1}{m_3}$ are approximately equal to one for neutrino mass matrices of class B. So, neutrino mass matrices of class B give quasi-degenerate spectrum of neutrino masses. For neutrino mass matrices of class B, the ratio $\frac{m_1}{m_2}$, upto first order in s_{13} , is given by

$$\begin{aligned}
 B_1 & : \quad \frac{m_1}{m_2} = 1 + \frac{c_{23}}{c_{12}s_{12}s_{23}^3} s_{13} \cos \delta ; \\
 B_2 & : \quad \frac{m_1}{m_2} = 1 - \frac{s_{23}}{c_{12}s_{12}c_{23}^3} s_{13} \cos \delta ; \\
 B_3 & : \quad \frac{m_1}{m_2} = 1 - \frac{c_{23} \tan^2 \theta_{23}}{c_{12}s_{12}s_{23}^3} s_{13} \cos \delta ; \\
 B_4 & : \quad \frac{m_1}{m_2} = 1 + \frac{s_{23} \cot^2 \theta_{23}}{c_{12}s_{12}c_{23}^3} s_{13} \cos \delta ; \tag{26}
 \end{aligned}$$

Since, the mass ratio $\frac{m_1}{m_2}$ is always smaller than one, we find that $\cos \delta$ should be negative for B_1 and B_4 and positive for B_2 and B_3 , a result that can be gainfully used to distinguish

C.L.		M_{ee}	J
1	$2:0^0-2:0^0$	0:064eV	0:025-0:025
2	$7:7^0-7:7^0$	0:037eV	0:036-0:036
3	22^0-22^0	0:023eV	0:045-0:045

Table 5: The predictions for neutrino mass matrices of class B.

between mass matrices of class B. Hence, B_1 and B_4 (or B_2 and B_3) will have identical predictions for θ_{12} . Similarly, it can be seen that B_1 and B_3 (or B_2 and B_4) will have, almost, identical predictions for θ_{23} if it is near maximality. However, B_1 and B_4 (or B_2 and B_3) can be distinguished from each other by their predictions for the octant of θ_{23} and B_1 and B_3 (or B_2 and B_4) can be distinguished from each other by their predictions for the quadrant of θ_{12} . Thus, the four-fold degeneracy in class B is, now, lifted. Moreover, it follows from Eqs. (26) that the second term should be suppressed by $s_{13} \cos \delta$ if neutrino mass spectrum is quasi-degenerate ($m_1 \approx m_2$). For large θ_{13} , the Dirac phase should be peaked around 90° or 270° to keep the term $s_{13} \cos \delta$ small. However, for small θ_{13} , no additional constraint on δ is obtained. The fact that $\cos \delta$ should be negative for B_1 and B_4 type mass matrices and positive for B_2 and B_3 type mass matrices for the correct sign of m_{12}^2 results in the elimination of two quadrants of δ for each of these subgroups irrespective of the values of the oscillation parameters and their errors. In fact, the earlier analyses [2, 3] do not constrain the Dirac phase at all for these subgroup of mass matrices. In the analysis by Xing [2], the mass ratios $\frac{m_1}{m_3}$ and $\frac{m_2}{m_3}$ were examined and this important constraint on δ coming from the mass ratio $\frac{m_1}{m_2}$ was completely missed as a result. Another detailed numerical analysis by Guo and Xing [3] based upon R defined in Eq. (25) does not make use of the solar mass hierarchy as a result of which no constraints on δ were obtained for neutrino mass matrices of class B.

Now, we present the numerical results of our analysis for mass matrices of class B. The allowed range of δ is $(90^\circ - 270^\circ)$ for types B_1 and B_4 and $(-90^\circ - 90^\circ)$ for types B_2 and B_3 . In other words, $\cos \delta$ is negative for types B_1 and B_4 and positive for types B_2 and B_3 , as expected. This important result is valid irrespective of the ranges of the neutrino oscillation parameters entering in the analysis and is a consequence of the fact that the sign of m_{12}^2 is positive. If $\theta_{23} < 45^\circ$, B_1 and B_3 give normal hierarchy while B_2 and B_4 give inverted hierarchy. Similarly, if $\theta_{23} > 45^\circ$, then B_1 and B_3 give inverted hierarchy while B_2 and B_4 give normal hierarchy. Again, this important result is true irrespective of the values of the neutrino oscillation parameters (and their errors) and follows from the dependence of mass ratio $\frac{m_1}{m_3}$ on $\tan^2 \theta_{23}$ [cf. Table 2]. As noted earlier, the four types of neutrino mass matrices within class B differ in their predictions for θ_{12} and θ_{23} . There is no lower bound on θ_{13} in class B. The Majorana-type CP-violating phase ϕ , also, remains unconstrained. The predictions for θ_{12} , M_{ee} and J for class B mass matrices have been summarized in Table 5. These quantities are the same for mass matrices of types B_1, B_2, B_3 and B_4 . It can, also, be seen that θ_{12} is restricted to a very small range around zero and definite lower bounds on M_{ee} are obtained. It is important to note that $\theta_{23} = 45^\circ$ is disallowed for mass matrices of class B.

In Fig. 3, the correlation plots for all eight possible cases of B type mass matrices (B_1 , B_2 , B_3 and B_4 with normal as well as inverted hierarchy) have been shown for θ_{13} , m_1 , M_{ee} and J . These plots show that B type mass matrices exhibit eightfold degeneracy in the sense that eight different types of mass matrices have identical predictions for these parameters. Figures 3(a-d) depict the correlations of θ_{13} , J and M_{ee} with m_1 . It can be seen from Fig. 3(a) that an upper bound on θ_{13} constrains m_1 to a very narrow range. Even at three standard deviations, the allowed range of m_1 is 22° \pm 2° [cf. Table 5]. However, no constraints are obtained on the Majorana phase α [Fig. 3(b)]. The correlation plot of J with θ_{13} shows a linear behaviour which is a consequence of θ_{13} being small and δ being near 90° or 270° for most of the allowed neutrino parameter space. Since, $M_{ee} \propto m_1$, we give the correlation plots for M_{ee} instead of m_1 in Fig. 3(d) where it can be seen that the absolute neutrino mass scale and 1-3 mixing angles are anti-correlated with each other. Next, we depict the correlations of the quantities M_{ee} and J with the Majorana phases α and β in figures 3(e-h). The effective Majorana mass M_{ee} diverges at $\alpha = 0$ and $\beta = 0$ and so these points are not allowed. A lower bound on M_{ee} is required to constrain the Majorana phase α which, otherwise, remains unconstrained for mass matrices of class B [Fig. 3(f)]. It can be seen from Fig. 3(g) that J and α are directly correlated with each other. This is due to the fact that θ_{13} is constrained to a very narrow range around zero degree so that $\sin \theta_{13} \approx \theta_{13}$. The correlation between the two Majorana phases α and β is depicted in Fig. 3(i) which shows that α will be nearly zero for large β and vice-versa. Fig. 3(j) depicts the correlation between J and M_{ee} . One can see that maximal CP-violation is possible near the lowest possible value of M_{ee} in class B. It may be worthwhile to mention that the earlier analysis [3] fails to obtain any constraints on the ranges of CP-violating phases (α , β and δ) for the reasons discussed earlier.

Fig. 4 depicts the correlations which lift the degeneracy between the neutrino mass matrices of types B_1 (B_4) and B_2 (B_3). Since, the range of Dirac-type CP-violating phase, δ , is different for B_1 (B_4) and B_2 (B_3), the eightfold degeneracy in B type mass matrices has, now, been reduced to four-fold. The left panel depicts the correlation plots for both B_1 and B_4 and the right panel depicts the correlation plots for B_2 and B_3 . It can be seen from Fig. 4(a,b) that the range of Dirac-type CP-violating phase, δ , is 90° \pm 270° (90° \pm 90°) for B_1 and B_4 (B_2 and B_3) type mass matrices, as expected. Also, there is a strong correlation between Majorana-type CP violating phase, α , and Dirac-type CP-violating phase, δ , reinforcing the zeroth order result $\alpha + \delta = n + \frac{1}{2}$ given in Table 2. It can be seen from Fig. 4(c,d) that θ_{13} remains unconstrained in all cases because full range of θ_{13} is allowed at $\delta = 90^\circ$ and 270° . However, as we deviate from these values of δ , θ_{13} decreases rapidly to very small values. So, if the CP violation is found to be non-maximal, θ_{13} will be constrained to very small values. However, if CP violation is found to be nearly maximal, θ_{13} can be large. Thus, the suppression factor $s_{13} \cos \delta$ in the first order correction term in the Taylor expansion for $\frac{m_1}{m_2}$ is small as expected from the zeroth order approximation for this class.

Fig. 5 depicts the correlations of M_{ee} and θ_{23} with θ_{13} . The correlation plots with θ_{23} can be used to further reduce the remaining four-fold degeneracy in B type mass matrices to a two-fold degeneracy which will be lifted by the determination of the neutrino mass hierarchy. The left panel (right panel) depicts the correlation plots for B_1 (NH) and B_2 (IH) (B_1 (IH))

		J	M_{ee}
1	14^0-14^0	$0.024-0.024$	0.016 eV
2	16^0-16^0	$0.034-0.034$	0.013 eV
3	18^0-18^0	$0.045-0.045$	0.009 eV

Table 6: The predictions for θ_{23} , J and M_{ee} for neutrino mass matrices of class C.

and B_2 (NH)). The correlation plots of M_{ee} and θ_{23} with θ_{13} for B_3 (NH) and B_4 (IH) (or B_3 (IH) and B_4 (NH)) will be, almost, identical to the plots given in Fig. 5 because B_1 and B_3 (or B_2 and B_4) have, almost, identical predictions for θ_{23} and, therefore, are not given here. It can be seen from Fig. 5(a,b) that the effective Majorana mass M_{ee} is strongly correlated with θ_{23} . Moreover, maximal value of θ_{23} is not allowed by the current neutrino oscillation data since M_{ee} diverges at $\theta_{23} = \frac{\pi}{4}$. Larger the deviation of θ_{23} from maximality, smaller is the value of M_{ee} . Also, a large value of θ_{13} implies large deviations of θ_{23} from maximality. The extent of the deviation of 2-3 mixing from maximality is governed by the magnitude of the upper bound on M_{ee} while the direction of the deviation from maximality is governed by the quadrant of θ_{13} and the neutrino mass hierarchy.

4.3 Class C

It can be seen from Table 2 that the mass ratio $\frac{m_1}{m_2}$ is greater than one at zeroth order. However, the higher order terms in the Taylor series expansion of the ratio $\frac{m_1}{m_2}$ may make it smaller than one. Detailed numerical analysis shows that this actually happens and the mass matrices of class C are marginally allowed. The Taylor series expansion for $\frac{m_1}{m_2}$ to first order in s_{13} is given by

$$\frac{m_1}{m_2} = \frac{1}{\tan^2 \theta_{12}} \left[1 - \frac{\tan 2\theta_{23}}{s_{12}c_{12}} s_{13} \cos \delta \right] \quad (27)$$

For $\frac{m_1}{m_2}$ to be smaller than one, the term $(\tan 2\theta_{23} \cos \delta)$ should be positive. Therefore, when $\theta_{23} < 45^\circ$, we must have $90^\circ < \delta < 90^\circ$. Similarly, when $\theta_{23} > 45^\circ$, we must have $90^\circ < \delta < 270^\circ$. Just like class B, the correlation between the octant of θ_{23} and the quadrant of δ obtained here for class C is independent of the ranges of the neutrino oscillation parameters and is a generic feature of two texture zero mass matrices. The points $\theta_{13} = 90^\circ, 270^\circ$ and $\theta_{13} = 0^\circ$ are not allowed because the first order correction term vanishes at these points. The mixing angle θ_{23} should approach 45° as θ_{13} approaches 90° or 270° and θ_{13} approaches 0° so that the term $(s_{13} \tan 2\theta_{23} \cos \delta)$ can make the ratio $\frac{m_1}{m_2}$ smaller than one. The mass ratio $\frac{m_1}{m_3}$ is greater than one at the zeroth order. Therefore, neutrino mass matrices of type C may be expected to be consistent with inverted hierarchy only. However, we shall see in the detailed numerical analysis that the normal hierarchy is, also, allowed marginally.

Formass matrices of type C, with inverted hierarchy, the allowed ranges for the parameters θ_{13} , J and M_{ee} are given in Table 6. All other parameters remain unconstrained. The correlation

plots between various parameters have been depicted in Figs. 6-8. In Fig. 6, we have given the correlations of δ , θ_{13} , θ_{23} , M_{ee} and J with α . As discussed earlier, the values $\alpha = 90^\circ$ and 270° are not allowed [Fig. 6(a)]. Therefore, maximal CP-violation is not allowed for mass matrices of class C. For the maximal values of δ , α should be equal to zero. Therefore, the point $\alpha = 0^\circ$ is, also, not allowed. However, all other values of α are allowed. It can be seen from Fig. 6(b) that the Majorana phase β is a periodic function of α with a period of 180° and β can be zero at $\alpha = 0^\circ$ or 180° . However, the points $(\alpha = 0^\circ, \beta = 90^\circ)$ and $(\alpha = 0^\circ, \beta = 270^\circ)$ are disallowed. The correlation between δ and θ_{13} has been depicted in Fig. 6(c). The correlation between δ and θ_{23} has been depicted in Fig. 6(d) where it can be seen that the maximal 2-3 mixing is not allowed. However, the mixing angle θ_{23} will be below maximality if $\cos \delta$ is positive ($90^\circ-90^\circ$) and above maximality if $\cos \delta$ is negative ($90^\circ-270^\circ$). These conclusions are, completely, in agreement with the results obtained from the Taylor series expansion. Fig. 6(e) depicts the correlation between M_{ee} and α which yields a lower bound of about 0.02 eV on M_{ee} for $\alpha = 0^\circ$ or 180° for neutrino mass matrices of class C. As α deviates from the values 0° and 180° , M_{ee} increases and diverges as α becomes maximal. The correlation between J and α has been shown in Fig. 6(f).

In Fig. 7, we have shown the correlations of δ , θ_{23} and J with θ_{13} . In Fig. 7(a), (θ_{13}, δ) correlation has been depicted. Full range ($90^\circ-90^\circ$) for δ is allowed for $\theta_{13} = 0$. However, it can be seen from Fig. 7(a) that a lower bound on θ_{13} of about 4° will constrain δ to the range ($65^\circ-65^\circ$). As noted earlier, δ is, already, constrained to a small range around zero. However, it can be seen from Fig. 7(b) that δ can be further constrained if θ_{13} is found to be larger than 3° . A lower bound on θ_{13} larger than 3° will disallow a finite range of δ around zero. From the $(\theta_{13}, \theta_{23})$ correlation plot [Fig. 7(c)], it can be seen that larger the value of θ_{13} , larger will be the deviation of θ_{23} from maximality. The point $(\theta_{13} = 0^\circ, \theta_{23} = 45^\circ)$ is not allowed. The disallowed range of θ_{23} around 45° increases with increase in θ_{13} . For example, the disallowed range of θ_{23} at $\theta_{13} = 6^\circ$ is approximately $44^\circ-46^\circ$. For small values of θ_{13} , J is proportional to θ_{13} and the constant of proportionality is determined by $\sin \delta$ [cf. Eq. (23)]. These features can be seen graphically in the correlation plot between J and θ_{13} depicted in Fig. 7(d).

Some other important correlation plots have been shown in Fig. 8. It can be seen from the (δ, β) correlation plot [Fig. 8(a)] that the two Majorana phases can not vanish simultaneously. The correlation between M_{ee} and δ has been shown in Fig. 8(c) where it can be seen that an upper bound on M_{ee} will reject a considerable range of δ . The (M_{ee}, β) correlation plot has been given in Fig. 8(d). It can be seen that the allowed range of β (which is $15^\circ-15^\circ$ for small values of M_{ee}) can be further constrained if M_{ee} is found to be larger than 0.03 eV. Fig. 8(e) depicts the correlation between M_{ee} and θ_{23} . It can be seen that M_{ee} diverges for maximal 2-3 mixing. A lower bound on M_{ee} can be used to constrain θ_{23} .

For C type mass matrices, with normal hierarchy Dirac-type CP-violation phase, δ , can have only two values $\delta = 90^\circ$ or 180° . Majorana-type CP-violating phases (β and β') and θ_{13} remain unconstrained. There is a strong correlation between θ_{13} and θ_{23} in this case. Larger the allowed range of θ_{13} , larger will be the deviation of θ_{23} from maximality. The neutrino mass matrices of class C were examined analytically in [10] where some of the results reported here for class C have been obtained.

4.4 Eightfold degeneracy

The forthcoming neutrino experiments will aim at measuring the neutrino mass hierarchy, Dirac type CP violating phase and the deviations of the atmospheric mixing angle from maximality [19]. The results of these experiments will fall in one of the following eight categories of phenomenological interest:

1. NH, $\theta_{23} < 45^\circ$ and $90^\circ < \delta < 270^\circ$,
2. NH, $\theta_{23} > 45^\circ$ and $90^\circ < \delta < 90^\circ$,
3. NH, $\theta_{23} < 45^\circ$ and $90^\circ < \delta < 90^\circ$,
4. NH, $\theta_{23} > 45^\circ$ and $90^\circ < \delta < 270^\circ$,
5. IH, $\theta_{23} > 45^\circ$ and $90^\circ < \delta < 270^\circ$,
6. IH, $\theta_{23} < 45^\circ$ and $90^\circ < \delta < 90^\circ$,
7. IH, $\theta_{23} > 45^\circ$ and $90^\circ < \delta < 90^\circ$,
8. IH, $\theta_{23} < 45^\circ$ and $90^\circ < \delta < 270^\circ$.

The eight cases given above are degenerate for the present neutrino oscillation data because of the octant degeneracy of θ_{23} (i.e. if $\theta_{23} < 45^\circ$ or $\theta_{23} > 45^\circ$), the intrinsic degeneracy in the sign of $\cos \delta$ and the two-fold degeneracy in the sign of m_{23}^2 . This degeneracy known as the eightfold degeneracy in the neutrino parameter space has been studied extensively in the literature [19, 20, 21, 22]. A specific project named Tokai-to-Kamioka-Korea (T2KK) two detector complex which will receive neutrino superbeams from J-PARC has been proposed [22] to resolve these degeneracies. The intrinsic degeneracy in the sign of $\cos \delta$ will be resolved by the spectrum information at T2KK and the degeneracy in the sign of m_{23}^2 will be resolved by observing the difference in the earth matter effects between the intermediate and far detectors. The θ_{23} octant degeneracy will be resolved by observing the difference in m_{12}^2 oscillation effects between the intermediate and far detectors at T2KK. In addition, neutrino factories [23] and beta-beam experiments [24] have the potential to resolve the eightfold degeneracy.

5 Conclusions

If neutrinoless double beta decay searches give positive results and M_{ee} is measured experimentally or the atmospheric/reactor neutrino oscillation experiments confirm inverted hierarchy, the neutrino mass matrices of class A will be ruled out. A generic prediction of this class of models is a lower bound on θ_{13} [Table 3]. If the forthcoming neutrino oscillation experiments measure θ_{13} below 3.3° , the neutrino mass matrices of class A will, again, be ruled out. If M_{ee} is found to be non-zero, the mass matrices of class B or C may be allowed. The eight different types of mass matrices in class B can be distinguished from one another

Categories	Degeneracies			Matrices		
	sign of m_{23}^2	sign of $\cos 2_{23}$	sign of \cos	A	B	C
1	+	+	-	A_2	B_1 (NH)	
2	+	-	+	A_1	B_2 (NH)	
3	+	+	+		B_3 (NH)	
4	+	-	-		\mathbb{B} (NH)	
5	-	-	-		\mathbb{B} (IH)	
6	-	+	+		B_2 (IH)	C (IH)
7	-	-	+		\mathbb{B} (IH)	C (IH)
8	-	+	-		\mathbb{B} (IH)	

Table 7: The consequences of resolving the eightfold experimental degeneracies for the neutrino mass matrices with two texture zeros.

by the future experimental data by the resolution of the eightfold degeneracy of the neutrino parameter space. The observation of correlations between various neutrino parameters like θ_{13} , θ_{23} , and M_{ee} etc. will confirm the neutrino mass matrices with two texture zeros. Moreover, the CP-violation in lepton number conserving and non-conserving processes will be correlated in a definite way and there will be only one independent CP-violating measure for both types of processes.

Main conclusions of the present study have been summarized in Table 7 which shows how the resolution of the degeneracies of neutrino parameter space will resolve the degeneracies of the neutrino mass matrices. As an illustration for the use of Table 7, we look at the results obtained for category 1 for which the signs of m_{23}^2 and $\cos 2_{23}$ are positive and the sign of \cos is negative. For this category, the neutrino mass matrices of type A_2 and B_1 (for normal hierarchy only) may explain the neutrino data whereas the mass matrices of class C are ruled out. Other possibilities summarized in Table 7 may be understood similarly. It is found that the degeneracies in the neutrino parameter space are inextricably linked to the degeneracies in the neutrino mass matrix and by finding the hierarchy, octant of θ_{23} and sign of \cos , the future experiments will settle the fate of neutrino mass matrices with two texture zeros. The resolution of the eightfold degeneracy in the neutrino parameter space will, also, resolve the eightfold degeneracy of the neutrino mass matrices of class B as can be seen from figures 4 and 5. Figures 4 and 5, also, illustrate the decoupling of degeneracies in the sense that two mass matrices can be degenerate in their predictions but may have different predictions for θ_{23} or vice-versa. A similar decoupling of degeneracies occur in neutrino oscillation experiments with matter effects [21] where an experiment may be insensitive to the sign of \cos but can resolve the degeneracy in the sign of $\cos 2_{23}$ or it can be insensitive to the sign of $\cos 2_{23}$ but can resolve the degeneracy in the sign of \cos .

6 Acknowledgments

The research work of S. D. and S. V. is supported by the Board of Research in Nuclear Sciences (BRNS), Department of Atomic Energy, Government of India vide Grant No. 2004/37/23/BRNS/399. S. K. acknowledges the financial support provided by Council for Scientific and Industrial Research (CSIR), Government of India. We would like to thank Manmohan Gupta for critical reading of the manuscript and helpful suggestions.

References

- [1] Paul H. Frampton, Sheldon L. Glashow and Danny Marfatia, *Phys. Lett. B* 536, 79 (2002); Bipin R. Desai, D. P. Roy and Alexander R. Vaucher, *Mod. Phys. Lett. A* 18, 1355 (2003).
- [2] Zhizhong Xing, *Phys. Lett. B* 530 159 (2002).
- [3] Wanlei Guo and Zhizhong Xing, *Phys. Rev. D* 67, 053002 (2003).
- [4] Alexander Merle and Werner Rodejohann, *Phys. Rev. D* 73, 073012 (2006); S. Dev and Sanjeev Kumar, hep-ph/0607048.
- [5] S. Dev, Sanjeev Kumar, Surender Verma and Shivani Gupta, hep-ph/0611313.
- [6] G. C. Branco, R. Gonzalez Felipe, F. R. Joaquim and T. Yanagida, *Phys. Lett. B* 562 265 (2003); Bhag C. Chauhan, Joao Pulido and Marco Picariello, *Phys. Rev. D* 73, 053003 (2006).
- [7] Xiao-Gang He and A. Zee, hep-ph/0302201 v2.
- [8] Suraj N. Gupta and Subhash Rajpoot, "Quark Mass Matrices and the Top Quark Mass", Wayne State University Preprint, September 1990; S. N. Gupta and J. M. Johnson, *Phys. Rev. D* 44, 2110 (1991); S. Rajpoot, *Mod. Phys. Lett. A* 7, 309 (1992); H. Fritzsch and Z. Z. Xing, *Phys. Lett. B* 353, 114 (1995).
- [9] P. H. Frampton, M. C. Oh and T. Yoshikawa, *Phys. Rev. D* 66, 033007 (2002).
- [10] Walter Grimus and Luis Lavoura, *J. Phys. G* 31, 693-702 (2005).
- [11] H. C. Goh, R. N. Mohapatra and Siow-Phang Ng, *Phys. Rev. D* 68, 115008 (2003).
- [12] S. Kaneko, M. Katsumata and M. Tanimoto, *JHEP* 0307, 025 (2003).
- [13] G. L. Fogli et al, hep-ph/0506083 v1.
- [14] M. Maltony, T. Schwetz, M. A. Tortola and J. W. F. Valle, hep-ph/0405172 v5.
- [15] J. Nelson, Talk at Neutrino 2006, 1319 June 2006, Santa Fe, New Mexico, <http://neutrinosantafe06.com>.

- [16] B. Aharmim et al. [SNO collaboration], Phys. Rev. C 72, 055502 (2005), [nucl-ex/0502021](#).
- [17] T. Araki et al. [KamLAND Collaboration], [hep-ex/0406035](#); Talk by G. Gatta at Neutrino 2004, 1419 June 2004, Paris, <http://neutrino2004.in2p3.fr>.
- [18] C. Jarlskog Phys. Rev. Lett. 55, 1039 (1985).
- [19] E. Abouzaid et al, Report of the APS Neutrino Study Reactor Working Group, 2004.
- [20] Hisakazu Minakata, Hiroshi Nunokawa, Stephen Parke, Phys. Rev. D 66, 093012 (2002).
- [21] Takaaki Kajita, Hisakazu Minakata, Shohei Nakayama, and Hiroshi Nunokawa, Phys. Rev. D 75, 013006 (2007).
- [22] Hisakazu Minakata, [hep-ph/0701070](#).
- [23] Raj Gandhi and Walter Winter, [hep-ph/0612158](#); A. M. Gago and J. Jones Perez, [hep-ph/0611110](#).
- [24] E. Fernandez-Martinez, [hep-ph/0605101](#); A. Donini and E. Fernandez-Martinez, Phys. Lett. B 641 432 (2006), [hep-ph/0603261](#).

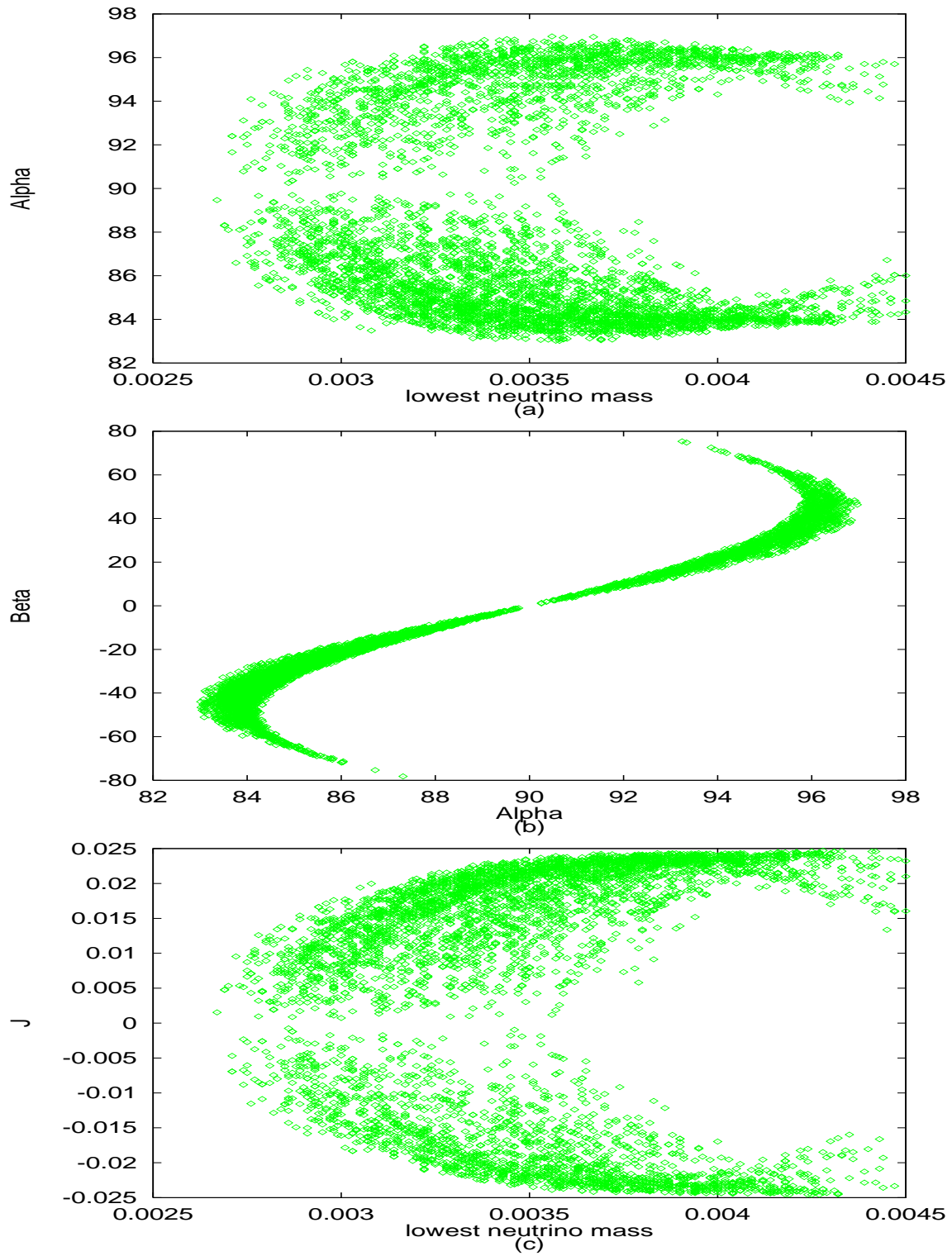


Figure 1: Correlation plots for neutrino mass matrices of class A at one standard deviation.

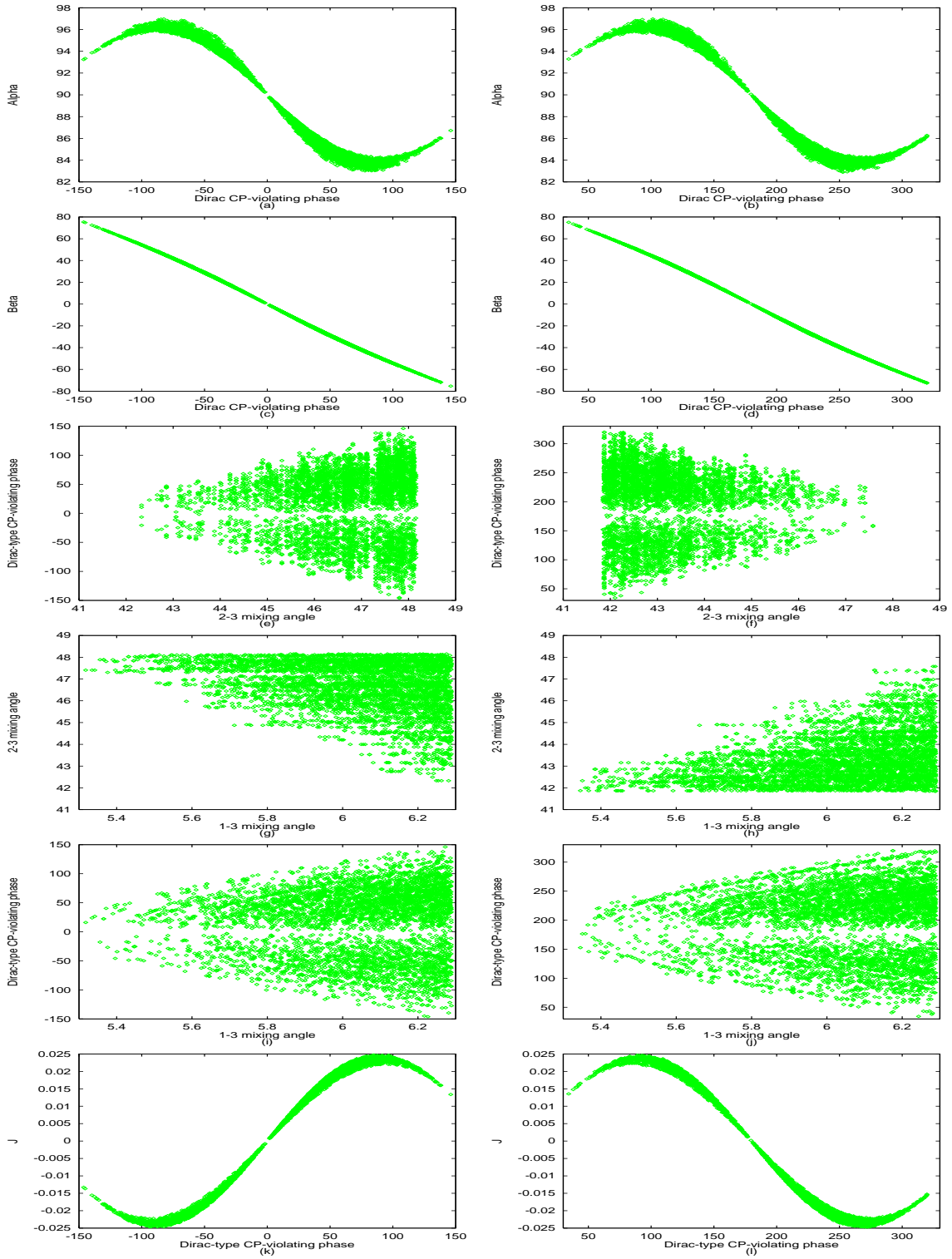


Figure 2: Correlation plots for neutrino mass matrices of type A_1 (left panel) and A_2 (right panel).

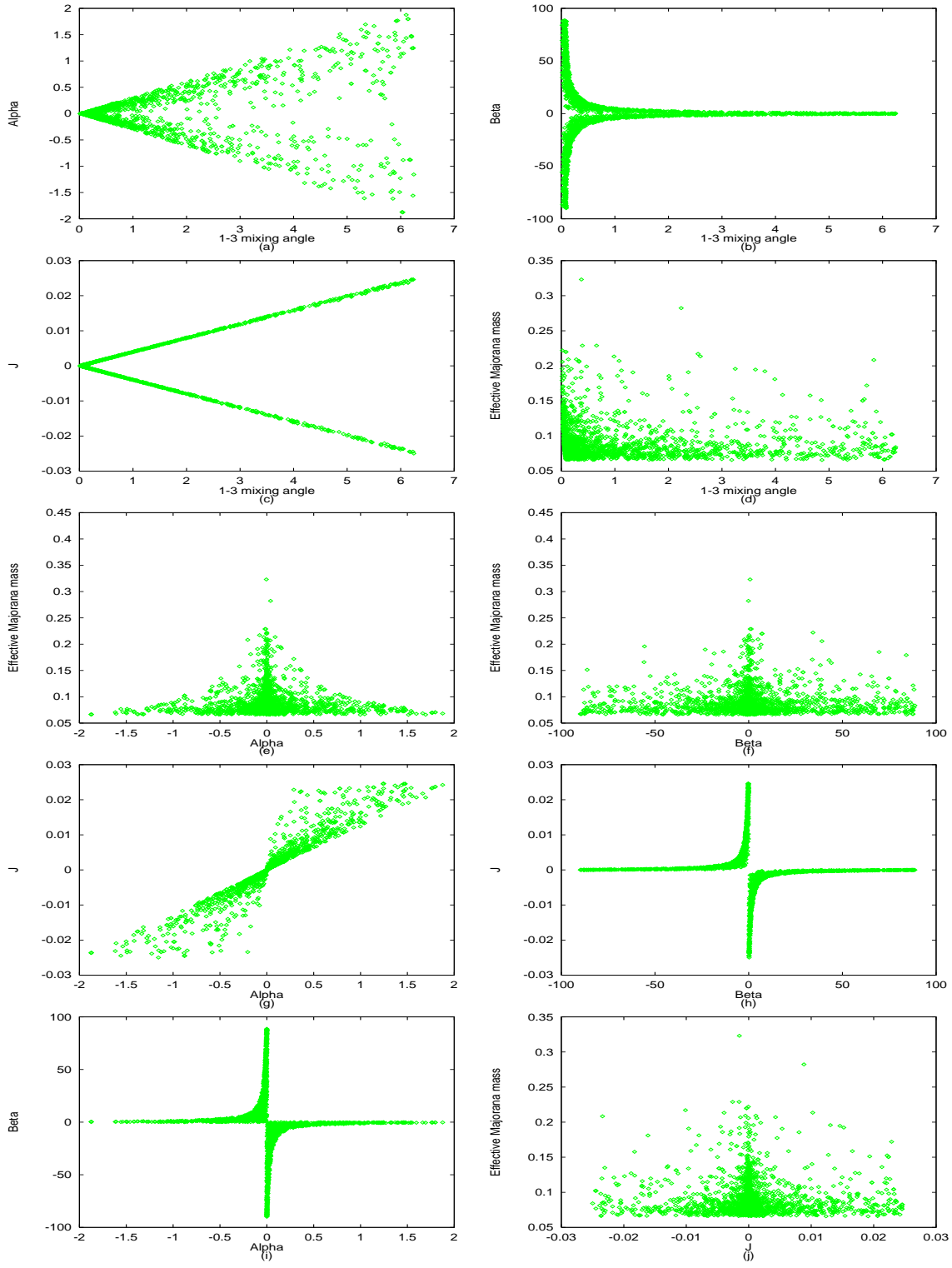


Figure 3: 1 correlation plots for B_1, B_2, B_3 and B_4 type mass matrices with normal as well as inverted hierarchies.

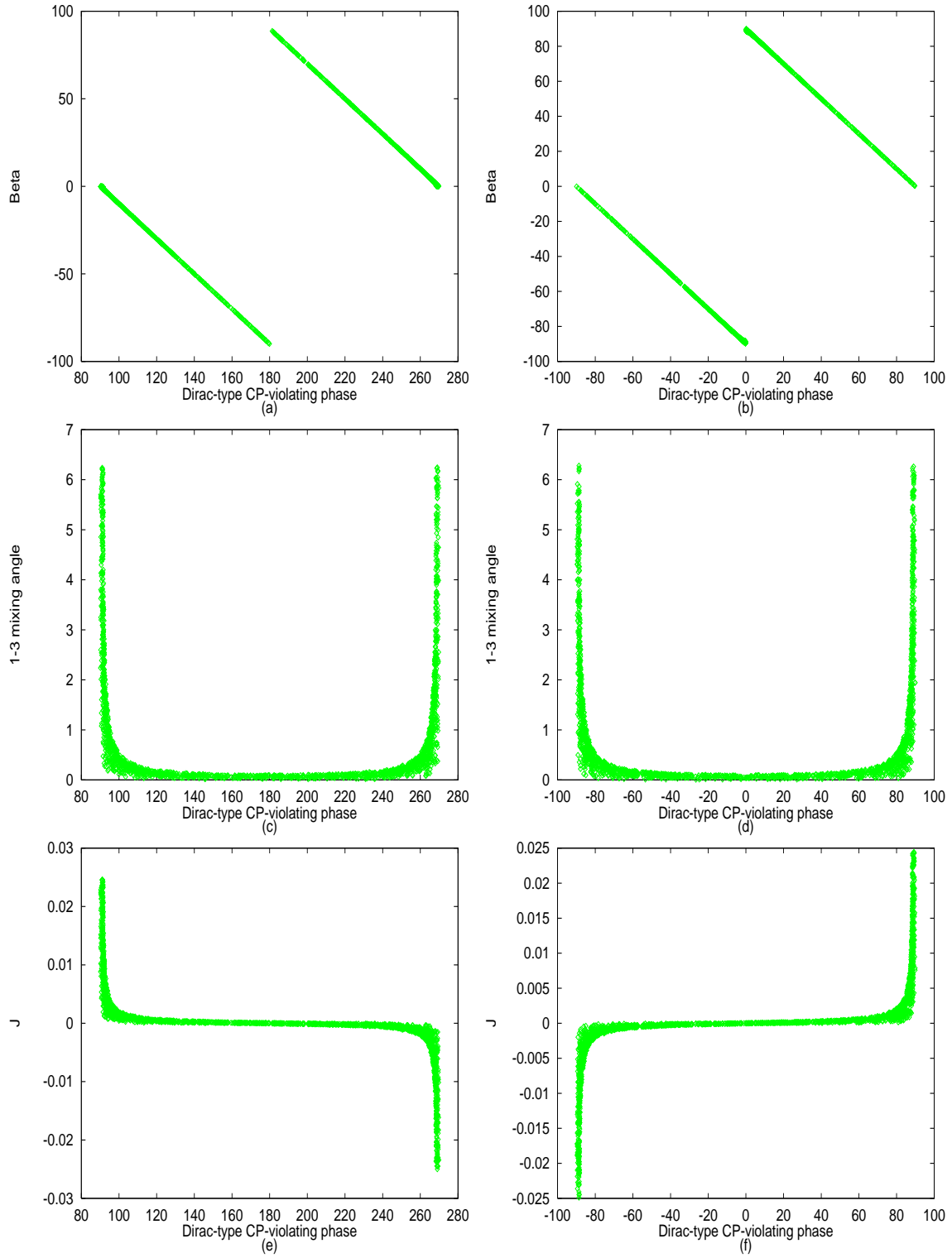


Figure 4: The left panel shows the correlation plots for B_1 or B_4 while right panel shows the correlation plots for B_2 or B_3 type mass matrices.

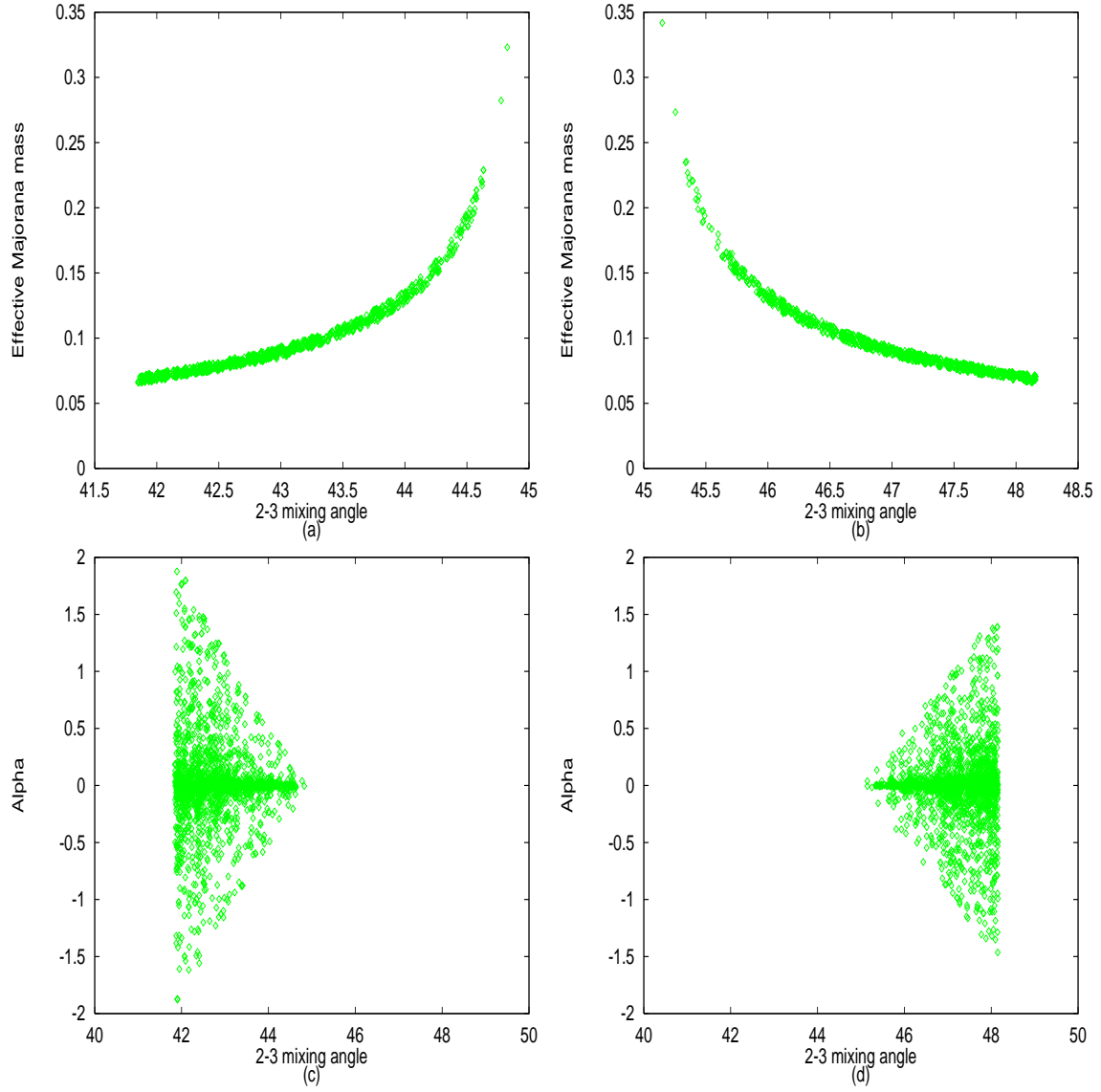


Figure 5: Variation of M_{ee} and α with θ_{23} . The left [right] panel plots are for B_1 (NH), B_2 (IH) [B_3 (IH), B_4 (NH)] type mass matrices.

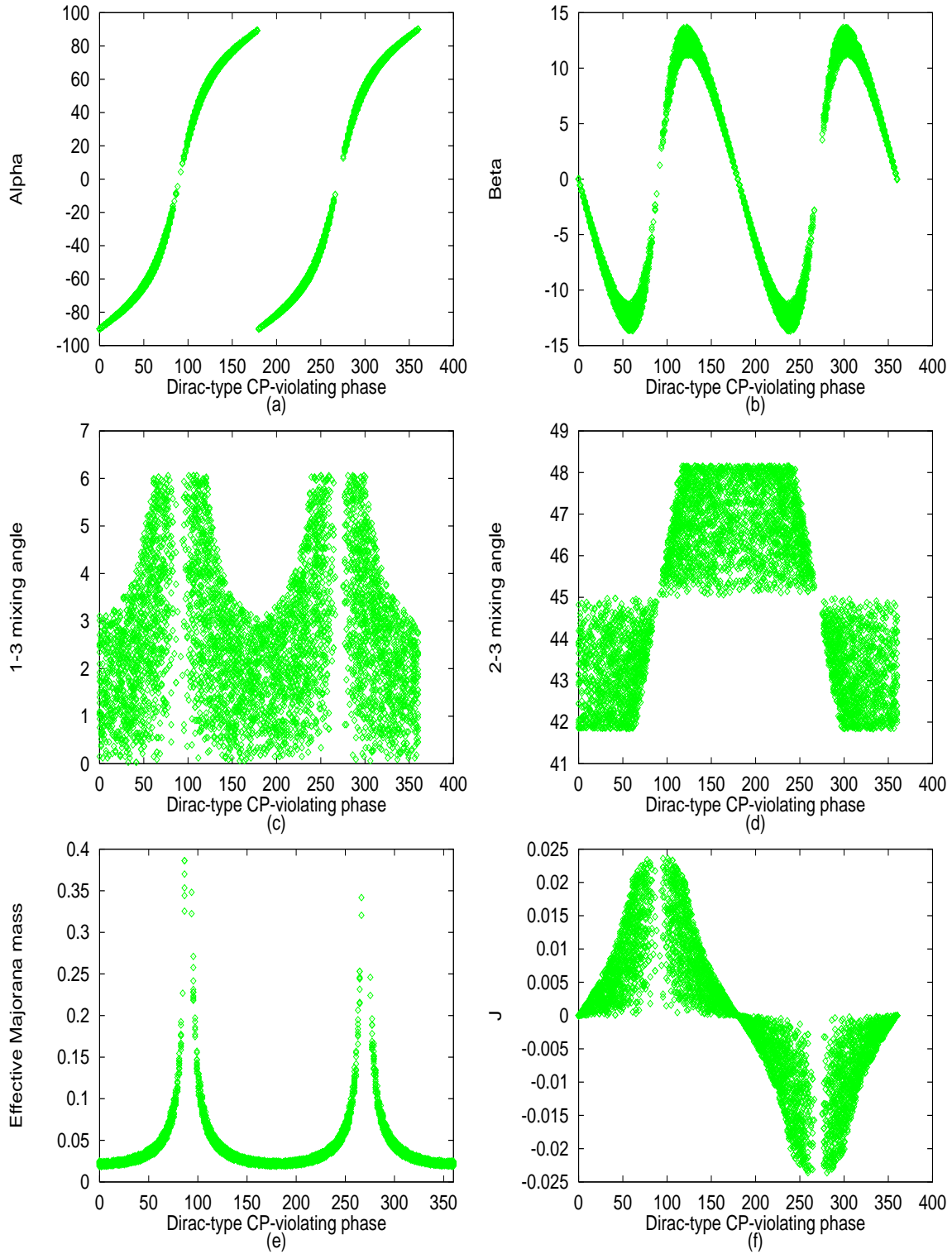


Figure 6: The correlation plots for CP-violating phase for neutrino mass matrices of type C with inverted hierarchy.

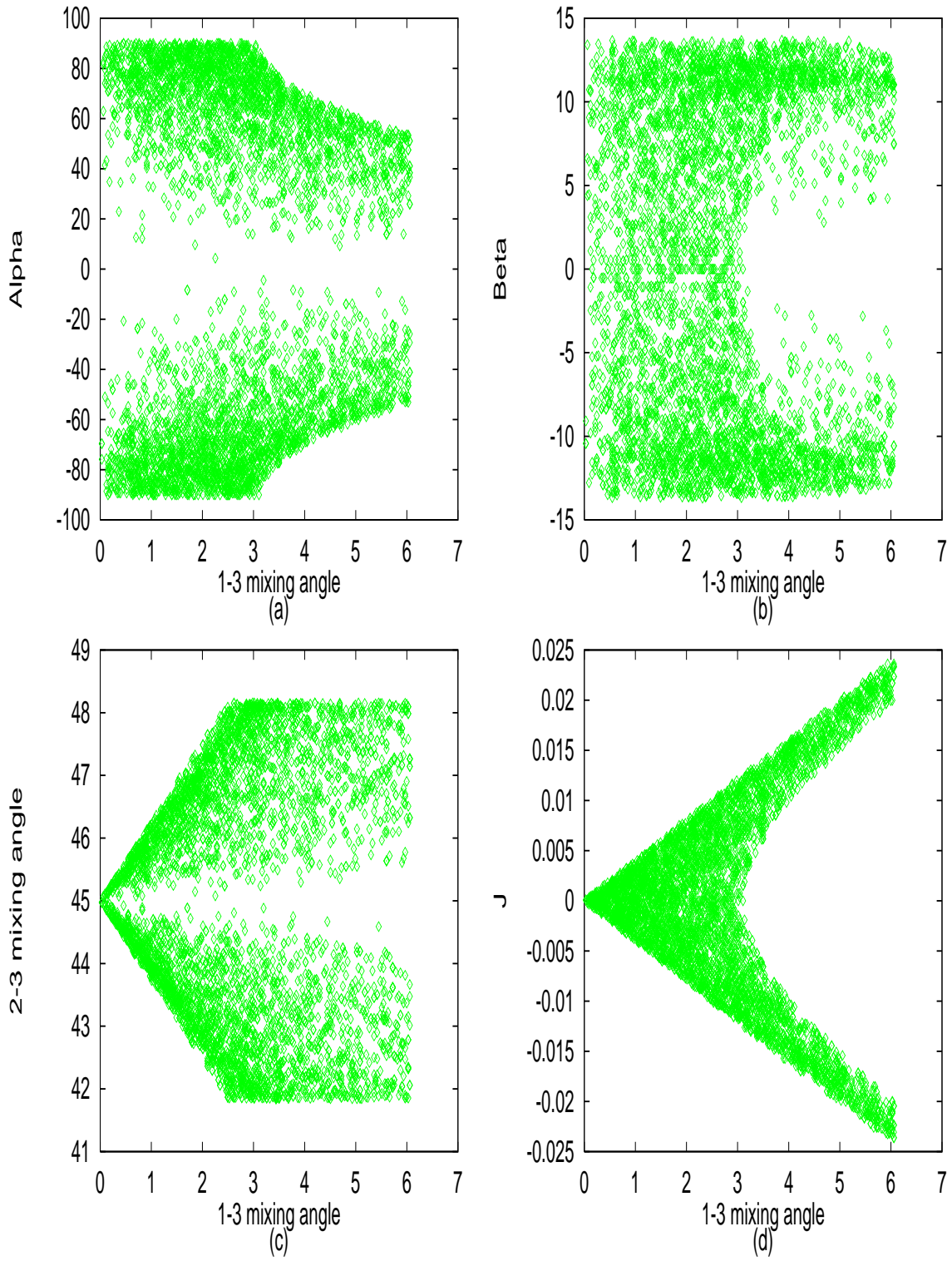


Figure 7: The correlation plots for the mixing angle θ_{13} for neutrino mass matrices of type C with inverted hierarchy.

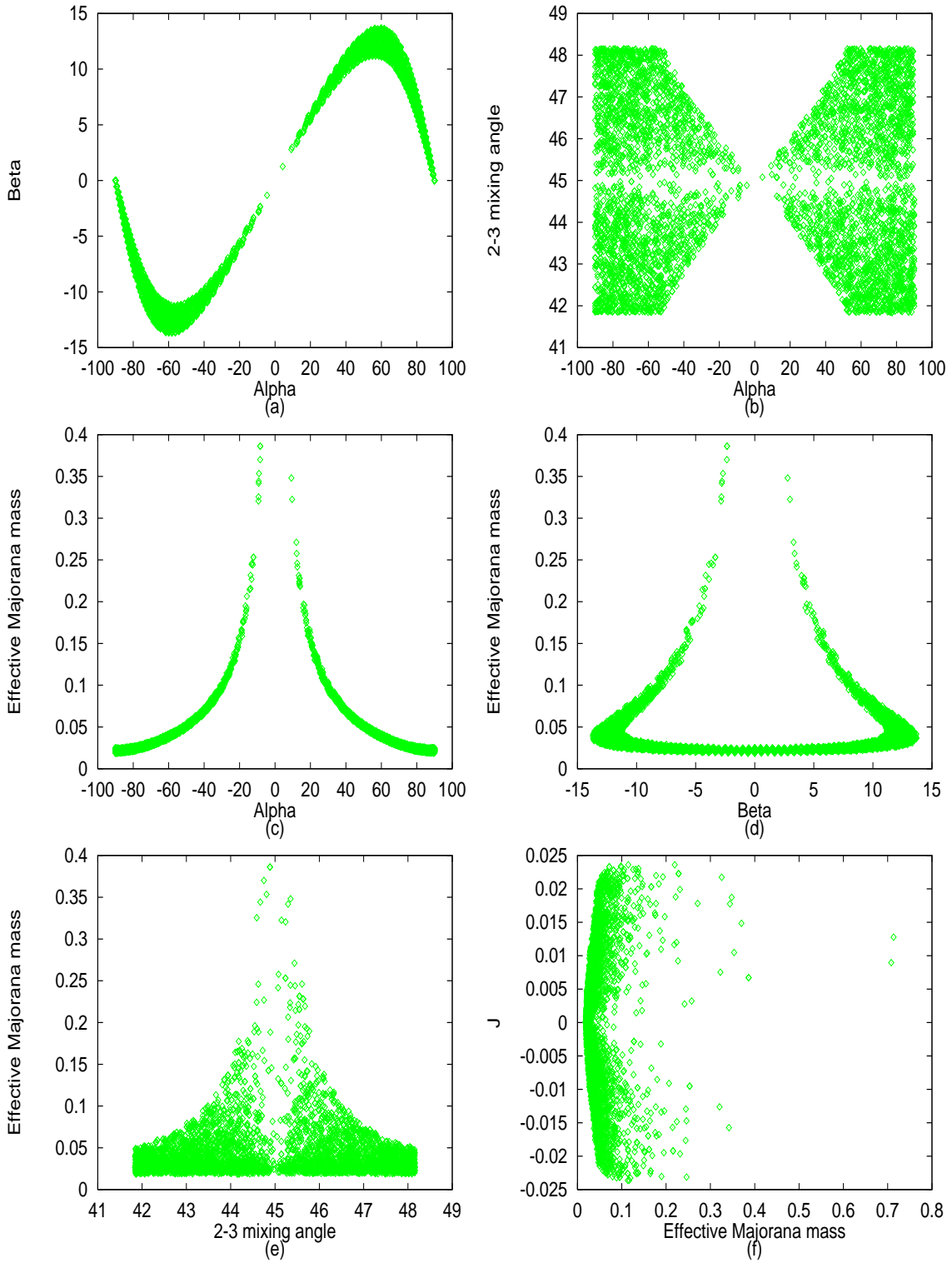


Figure 8: Some other important correlation plots for neutrino mass matrices of type C with inverted hierarchy.